AIAA JOURNAL
Vol. 39, No. 3, March 2001

Structure, Penetration, and Mixing of Pulsed Jets in Crossflow

Adnan Eroglu* and Robert E. Breidenthal†
University of Washington, Seattle, Washington 98195

Effects of periodic disturbances on the structure and mixing of a transverse jet have been investigated through chemically reactive laser-induced fluorescence experiments in a water model. Flow visualization experiments with a steady, round jet in crossflow revealed a distinct vortex loop merging pattern among the vortices that make up the curved shear layer around the jet. As the vortex loops are stretched and distorted, certain parts of the neighboring loops with the opposite or the same sign of vorticity merge, resulting in cancellation or intensification of the vorticity in the corresponding regions of the jet. When the flow rate of this jet was periodically modulated by a square wave, however, distinct vortex rings were created whose spacing and strength were dictated by the pulsing frequency for a given jet and crossflow combination. At low pulsing rates, these rings penetrated into the crossflow significantly deeper than the steady jet. An optimum pulsing frequency was found at which closely spaced vortex rings were observed, which penetrated as discrete vortices into the crossflow in the near field. Strong interactions among neighboring rings were observed farther downstream. Experiments with high Reynolds number jets revealed up to a 70% increase in jet penetration, whereas the flame length of the jet was reduced by 50% at this optimum pulsing frequency.

Nomenclature

c_f	=	flame or reaction chord length, $\sqrt{(x_f^2 + y_f^2)}$
d_j	=	nozzle exit diameter
f	=	pulsing frequency
Re_j	=	Reynolds number
Sr	=	Strouhal number, fd_j/U_j
U_j	=	jet velocity
U_∞	=	crossflow velocity
VR	=	mean jet-to-crossflow velocity ratio
x	=	streamwise coordinate
x_f	=	streamwise flame or reaction length
y	=	transverse coordinate
y_f	=	transverse flame or reaction length
α	=	duty cycle, percentage of jet-on during each cycle
ϕ	=	stoichiometric (equivalence) ratio

I. Introduction

A JET, introduced at large angles into a crossflow, is commonly utilized in various applications. A few of these include injection of gaseous or liquid fuel jets in a crossflowing airstream in a premixing burner, injection of dilution air through combustor liners, discharge of chimney gases into the atmosphere, and thrust control of rockets via small jets. In most of these applications, it is desirable to have control over the fluid mechanics of this flow to improve the quality of the end process. For example, entrainment of crossflow fluid into a fuel jet and the resulting mixing between the two streams are critical to the efficiency and size of a combustor, as well as to the composition of the combustion products. The mixing problem is more important for high-speed combustion applications; ultrafast mixing of fuel with the oxidizer is required in the engine of a scramjet, for which a transverse jet is a potential candidate due to slow mixing characteristics of mixing layers at supersonic speeds. On the other hand, recent studies have shown that production of pollutants, such as NO_x components, can be reduced by further understanding and improving the fluid mechanics of the combustion, that is, by reducing the duration of high-temperature exposure of the combustion gases.

It has long been recognized that a transverse jet is a more efficient mixer than a freejet or a mixing layer.[1,2] This enhanced mixing behavior of the transverse jet is generally attributed to a longitudinal, counter-rotating vortex pair, which gives a characteristic kidney shape to jet's cross section as sketched in Fig. 1. Consequently, a large portion of the research on this flow has been concentrated on this counter-rotating vortex pair, often neglecting the three-dimensional nature of the jet–crossflow interaction.

A different approach was taken in this study: First, extensive water-tunnel flow visualization experiments were conducted with a round transverse jet, in which the three-dimensional structure of the jet was analyzed. It was observed during these experiments that a curved shear layer, composed of distinct vortex loops, is formed around the jet in the very near field of the jet. However, contrary to the circular vortex rings in a freejet, the vortex loops of a transverse jet are distorted in a unique way out of their plane, such that the downstream side of each loop is forced to merge with the upstream side of either neighboring upstream or downstream loops, depending on the jet-to-crossflow velocity ratio. This mechanism causes a cancellation in vorticity at the crossflow side of the jet as parts of discrete loops with opposite sign of vorticity merge. Meanwhile, parts of each loop are distorted out of their own plane, forming two spirals on both sides of the jet, which merge with the spirals formed by the neighboring loops. This mechanism apparently causes the vorticity to intensify along two counter-rotating, streamwise vortex tubes as the parts of neighboring rings of the same sign merge.

Once the role of the shear layer vortex loops on the structure and mixing of a transverse jet was established, the question of how unsteady forcing would affect the formation and interaction of these vortex loops was raised. With this question in mind, the jet supply line was divided into two branches and a solenoid valve was placed in one of them. The flow rate was either partially or fully modulated by this valve, and the resulting changes in the structure, penetration, and flame length of the jet were investigated.

A recent study by Wu et al.[3] indicated that at low pulsing frequencies, a jet injected at 45 deg into a crossflow penetrates up to four times deeper than a steady jet for the same mean momentum flux. Our experiments[4] qualitatively confirm this finding for low Reynolds number jets, whereas the experiments conducted with high Reynolds number jets revealed a reduced, but still significantly large, effect on penetration due to pulsing. Additionally, flow visualization of the pulsed jet indicates that spacing of the vortex loops

Received 24 January 1999; revision received 28 September 2000; accepted for publication 3 October 2000. Copyright © 2000 by the American Institute of Aeronautics and Astronautics, Inc. All rights reserved.

*Research Assistant, Department of Aeronautics and Astronautics; currently Head of Combustion, GT24/GT26 Gas Turbine Development, Business Center Turbomachinery, ABB Alstom Power, CH 5401 Baden, Switzerland; adnan.eroglu@power.alstom.com. Member AIAA.

†Professor, Department of Aeronautics and Astronautics. Member AIAA.

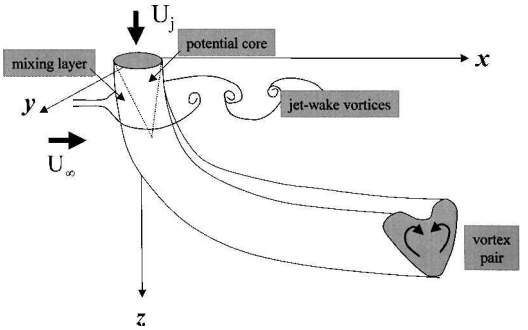

Fig. 1 Conventional description of turbulent jet in crossflow.

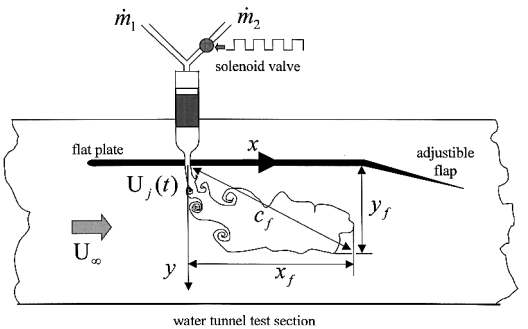

Fig. 2 Pulsed transverse jet flow geometry.

created by each pulse plays an important role in determination of the jet's penetration and flame length.

More recent investigations by Hermanson et al.[5] and Johari et al.[6] revealed similar trends in terms of penetration and mixing and shed light on the effect of varying the duty cycle of pulsation.

Furthermore, a dramatic change in the structure of the jet, splitting of the jet into two branches with one penetrating deep into the crossflow while the other one stays close to the wall where the jet is introduced, was observed in this study. This structure could be implemented in practical applications to utilize the existing vorticity in the jet's wake for the mixing of the two streams. The vorticity in the wake of the jet originally comes from the crossflow boundary layer.[7,8] This vorticity does not directly take part in jet's mixing with the crossflow for a steady jet because no jet fluid is shed into the wake region.

II. Experimental Facility and Techniques

Experiments were carried out in a horizontal-type recirculating water tunnel with a test section dimensions of $70 \times 70 \times 300$ cm. This facility, described in greater detail in Refs. 9 and 10, provided test section flow speeds up to 70 cm/s at a turbulence intensity of less than 0.3% of the flow speed.

The flow geometry is illustrated in Fig. 2. A pressurized air-driven setup supplies the jet fluid. This setup consists of a pressure tank and a distribution manifold, followed by two supply lines, each containing a regulating valve and a flowmeter. One of these lines contains a solenoid valve, which was used to introduce a periodic disturbance into the jet. The two supply lines merge before entering a nozzle apparatus, installed on a flat plate. The nozzle apparatus contains a foam section, a honeycomb, a straight settling section, and a contraction section of variable exit diameter. The flat plate, holding the nozzle apparatus, was installed 10 cm below water free surface. This plate is 70 cm wide and 130 cm long. A 5–1 aspect ratio elliptical leading edge and an adjustable flap at the trailing edge were used to control the crossflow boundary layer along the plate.

A square wave with duty cycle $\alpha = 50\%$, generated by a wave generator and amplified by a power supply, was used to pulse the solenoid valve. The finite response time of the solenoid valve, which was approximately 8 ms for the valve used, limited the maximum pulsing frequency that can be applied to the jet stream with this technique. Because of this limitation, pulsing frequency ranged from 0 to 20 Hz. However, this did not constitute a problem because the natural frequency of the curved shear layer around the jet falls within this range for the experiments reported here.

The jet fluid was either fully supplied through the solenoid valve or only a certain portion of it was passed through the solenoid valve, as the remaining portion was supplied from the second (undisturbed) line to analyze both large and small disturbance cases.

Laser-induced fluorescence was used to observe selected cross sections of the jet. External flow structure was visualized by a fluorescein dye (disodium fluorescein), illuminated by spotlights. An acid–base reaction yielded the flame length, defined as the location where all injected fluid has achieved a prescribed volumetric mixture ratio. A pH indicator, phenolphtalein, was added to the alkaline jet fluid to give a purple color to the jet stream. On mixing of the two streams to an equivalence ratio, preselected by the pH values of the jet and tunnel fluids, the purple color of the pH indicator becomes invisible, marking the flame or the mixing length.

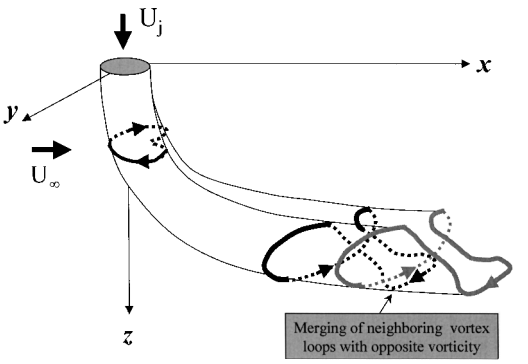

Fig. 3 Sketch of a steady transverse jet, illustrating the deformation and merging of the vortex loops; arrows in vortex loops represent the sign of vorticity.

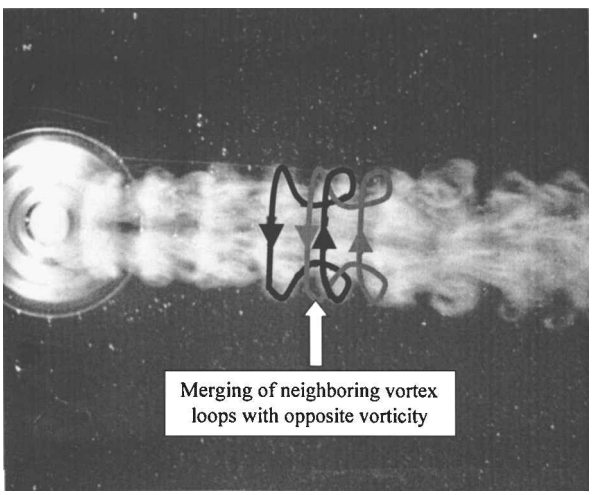

Fig. 4 Plan view of a steady transverse jet with $Re_j = 650$ and VR = 2.3, with sketches of distorted vortex loops; arrows indicate the sign of vorticity.

III. Results and Discussion

A. Flow Structure

The three-dimensional structure of an unforced transverse jet is illustrated in Fig. 3, showing the distortion and interaction of the shear layer vortex loops that make up the jet. A photograph of the plan view of a low Reynolds number transverse jet is given in Fig. 4, as visualized by spotlight-induced fluorescence. In Fig. 4, the jet is issuing toward the viewer and the crossflow is from left to right.

Figures 3 and 4, presented as examples of several video recordings of flow visualization tests, suggest that each ring is distorted out of its plane such that the downstream portion of a ring (lee side) is stretched to merge with the upstream portion (pressure side) of the following ring. It appears that this mechanism brings together parts of neighboring rings of opposite sign of vorticity, as indicated

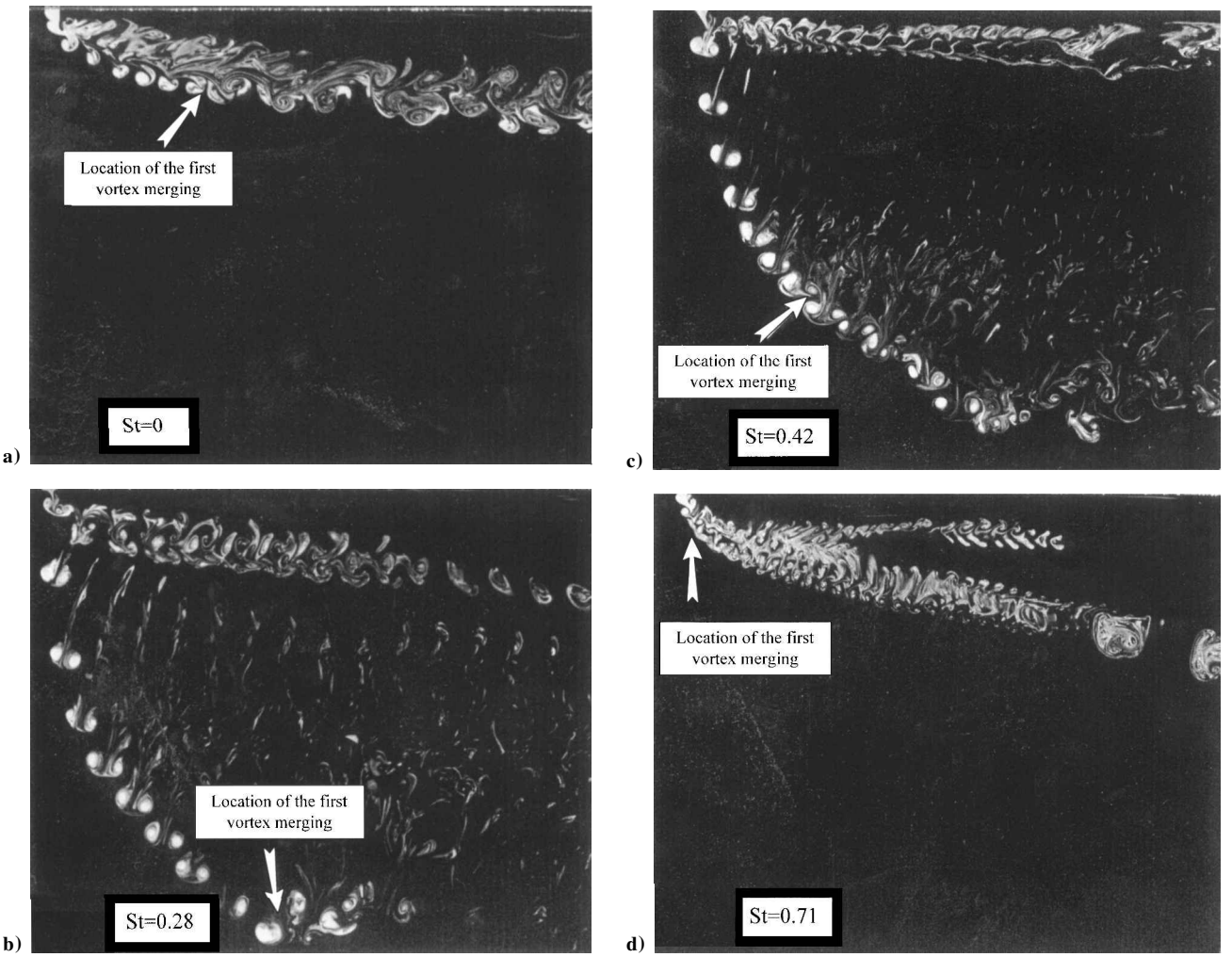

Fig. 5 Photographs of the streamwise cross section of a pulsed jet at Strouhal numbers of 0, 0.28, 0.42, and 0.71 for $Re_j = 650$ and VR = 2.3 (100% modulation).

with arrows in Fig. 3, resulting in cancellation of vorticity where this merging takes place. The remaining parts of each ring are spiraled into two counter-rotating vortices on both sides (which, for simplicity, are not included in Fig. 3) causing the jet vorticity to concentrate along a pair of longitudinal vortices.

Photographs of the side view of a low-Reynolds-number transverse jet, illuminated by a laser sheet at the streamwise symmetry plane, are given in Figs. 5a–5d for Strouhal numbers of 0, 0.28, 0.42, and 0.71, respectively. The jet Reynolds number Re_j is approximately 650, and mean jet-to-crossflow velocity ratio (VR) is 2.3. The unforced jet photograph (Fig. 5a) reveals the formation of a curved shear layer around the jet. In the near field, the aforementioned merging of the downstream side of each loop with the upstream side of the neighboring downstream loop can be seen along the lower surface of the jet, with an arrow indicating the location of the first vortex merging. The stretching and distortion of the loops can be seen in the wake side. In the far field, a more developed structure is present, which, in addition to merging of neighboring loops, also includes random pairings between neighboring loops.

When this jet is fully pulsed (100% modulation) at a rate of $Sr = 0.28$ (Fig. 5b) in a square wave, a dramatic change is observed in the overall structure of the jet: Two distinct branches are formed, one penetrating deep into the crossflow as the other one stays close to the wall. The lower branch consists of circular, undistorted vortex rings, which are spaced such that no pairing among neighboring rings can be seen until about 15 jet diameters from the nozzle exit in the crossflow direction. The upper branch also exhibits distantly spaced vortical structures, but they are more distorted. Jet fluid columns that appear to be stretched can be seen in the region between these two branches. Video recordings of the flow indicate that these columns connect the vortical structures in the two branches to each other: The ends of each column are connected to the centers of the corresponding vortex rings in the upper and lower branches.

As the pulsing rate is increased to $Sr = 0.42$ (Fig. 5c), the location where the first pairing is observed in the lower branch shifts upstream, to approximately eight jet diameters downstream from the nozzle exit. The upper branch also exhibits pairings within the observed area. As can be seen from Fig. 5d, increasing the pulsing rate to $Sr = 0.71$ causes the two-branched structure to largely disappear. Although the effects of pulsation on the formation of the vortical structures are clearly visible, the overall structure of the jet resembles the unforced case.

Photographs of a high-Reynolds-number transverse jet are given in Figs. 6a–6d for Strouhal numbers of 0, 0.04, 0.07, and 0.11, respectively. The jet Reynolds number and jet to crossflow velocity ratio, based on the mean jet velocity, are 6200 and 4.4, respectively, and flow is modulated 100% with a duty cycle of $\alpha = 0.5$.

The photographs given in Figs. 5 and 6 present certain similarities despite an order of magnitude increase in Reynolds number for the latter. In both cases, distinct vortical structures can be observed. A similar separation between these vortices and the body of the jet is observed. Thus, the experiments conducted at a low-Reynolds-number range provide useful visual information on the formation and interaction of the vortical structures that make up the flow. It is evident from Fig. 6 that at high Reynolds numbers flow structure gets more complicated, owing to significantly increased fine-scale turbulence.

At low pulsing rates, the jet exhibits distantly spaced vortex rings, which leave large amounts of fluid in their wake as they penetrate

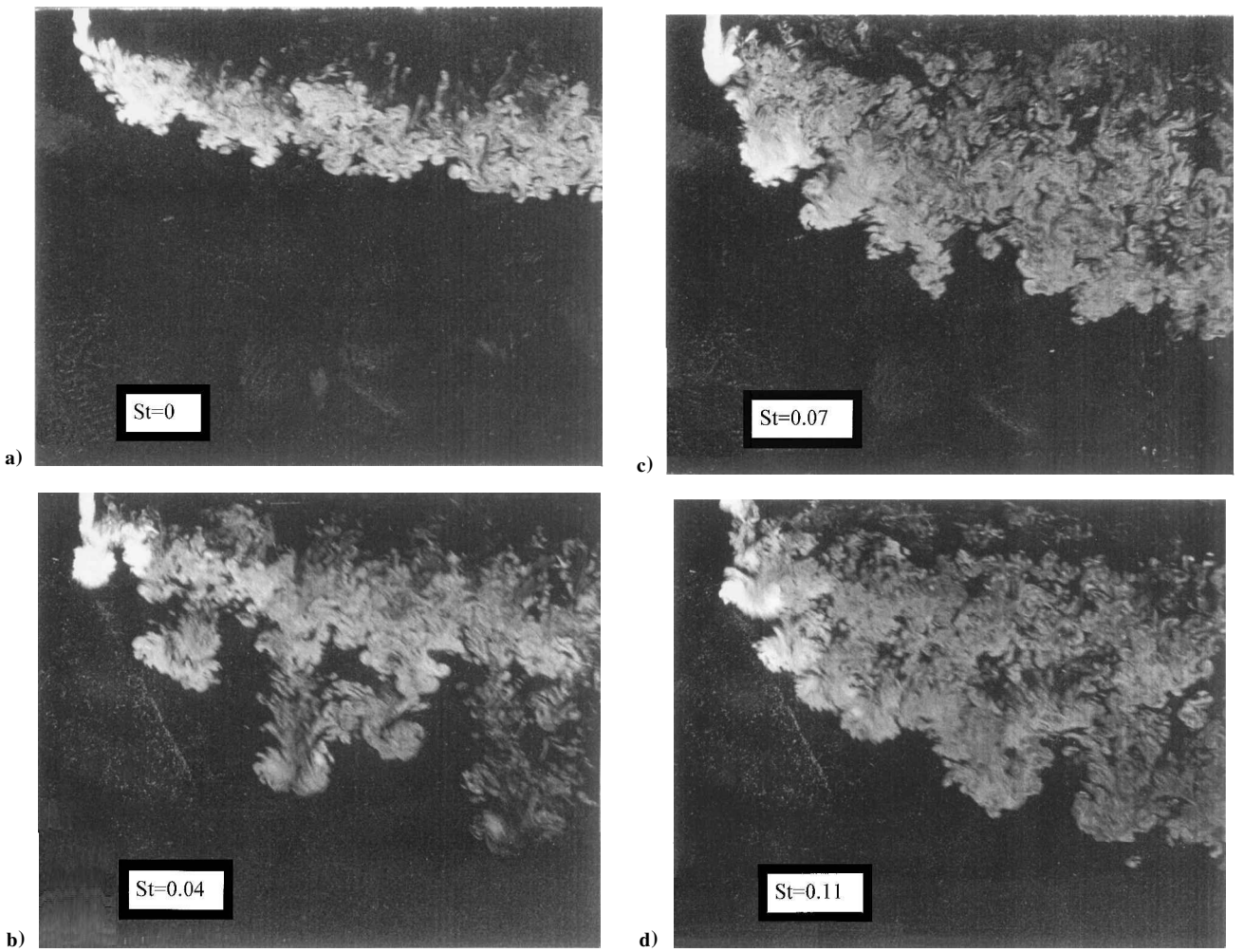

Fig. 6 Photographs of the streamwise cross section of a pulsed jet at Strouhal numbers of 0, 0.04, 0.07, and 0.11 for $Re_j = 6200$ and VR = 4.4 (100% modulation).

into the crossflow, as can be seen from Fig. 6b. At higher pulsing rates, these rings are spaced more closely. Strong interactions among neighboring rings result in a wide, uniformly mixed structure in the far field (Figs. 6c and 6d). It was observed that pulsing at a rate of beyond $Sr = 0.3$ did not change the overall structure of the jet significantly.

Modulating only 20% of jet's flow rate (small amplitude pulsing case) creates a similar effect on the flow structure, but, as described hereafter, the overall effect on penetration and mixing is smaller than the fully pulsed case.

B. Penetration

A sharp increase in the penetration, compared to the steady jet, is observed when the jet is pulsed at low frequencies ($Sr = 0.14$–0.42). At a distance of 40 jet diameters from the nozzle exit, the penetration of the $Sr = 0.28$ case is about 3.5 times greater than the steady jet for $Re_j = 650$ and VR = 2.3. As the pulsing rate is increased beyond $Sr = 0.7$, however, the penetration profile declines, approaching the steady jet case.

This observation is qualitatively similar to the data reported by Wu et al.[3] for a jet injected at 45 deg to the crossflow at VR = 4.7 and $Re_j = 470$. They suggest that the peaks in the time history of the pulsed jet's velocity are the major factors that cause this dramatic increase in the depth of penetration. In other words, because the mean flow rate of the jet is maintained constant, momentum of each pulse is greater than the momentum flux of the steady jet. Their hot film measurements indicate that the magnitude of the peak velocity decreases with increasing pulsing rate, having its maximum value at 1 Hz, the lowest pulsation rate tested in their study. They report only small oscillations around the mean value at 16 Hz. However, the photographs given in Fig. 6 suggest that an additional factor other

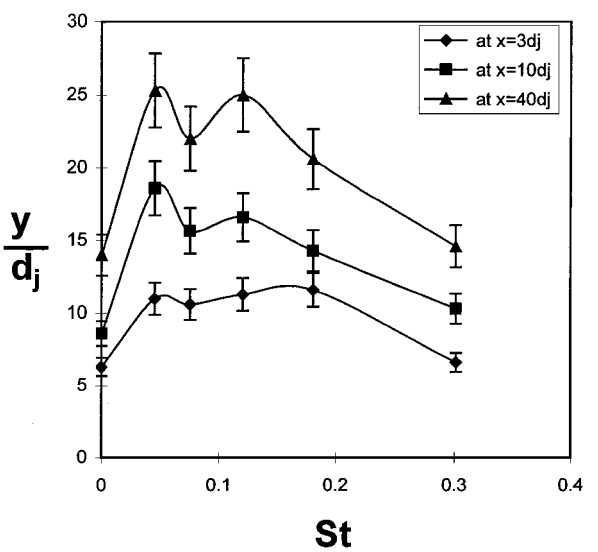

Fig. 7 Penetration depth variation with Strouhal number for Re_j = 6200 and VR = 4.4 (100% modulation).

than increased momentum of discrete pulses, namely, the spacing of the vortex rings generated due to pulsation, plays an important role in the penetration depth of the jet.

To further support this observation, the dependence of the penetration depth on the pulsing frequency is given in Figs. 7 and 8, for a fully (100%) and a partially (20%) modulated jet, respectively, at downstream distances of 3, 10, and 40 jet diameters from the nozzle exit. The jet Reynolds number and jet-to-crossflow VR, based on

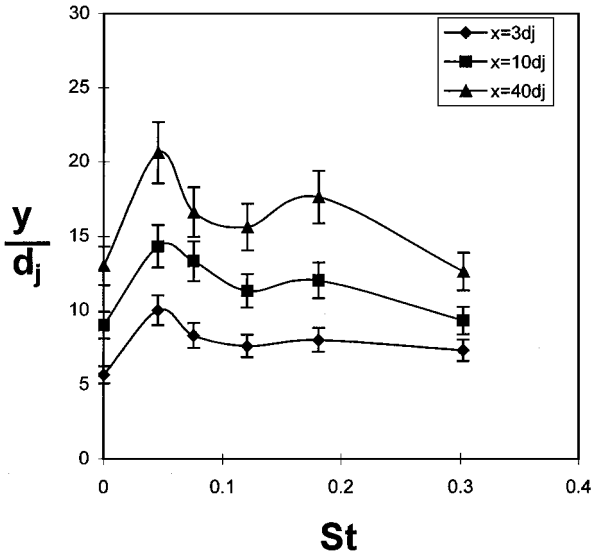

Fig. 8 Penetration depth variation with Strouhal number for Re_j = 6200 and VR = 4.4 (20% modulation).

the mean jet velocity, are 6200 and 4.4, respectively. There exist two peaks in penetration depth in both plots. As expected, the first peak is measured at the lowest pulsing rate of the tests conducted, where the momentum of each pulse is the maximum.

Surprisingly, despite the initial decline in penetration, increasing the pulsing rate to $Sr = 0.11$ for the fully modulated jet and to $Sr = 0.17$ for the 20% modulated jet causes the penetration depth to increase again. As can be seen from both plots, the maximum rise in penetration takes place in the far field, that is, at about $40d_j$ axial distance from the nozzle exit. For the fully pulsed jet, penetration depth at this location for the second peak is comparable to the first one.

Video recordings of the flow suggest strong interactions among closely spaced neighboring rings at the Strouhal number where the second peak is observed. In the near field, each ring penetrates into crossflow, partly by utilizing the induced velocity field of the ring downstream of it, that is, by traveling in its close wake region. In the far field, the sides of the neighboring rings merge, creating vortex pairs with opposite sign of vorticity, which evidently enhances penetration.

According to Pratte and Baines,[11] the trajectory for an unforced jet in crossflow is given by

$$y/(\mathrm{VR}\,d) = 2.05(x/\mathrm{VR}\,d)^{0.28} \tag{1}$$

To elucidate the effect of modulation, in Fig. 9 penetration data for the case of 100% modulation are presented in $y/(\mathrm{VR}\,d)$ vs $[x/(\mathrm{VR}\,d)]^{0.28}$ coordinates with Strouhal number as a parameter. As can be seen from Fig. 9, after accounting for the differences in VR, the pulsed jet has still significantly higher penetration than the non-pulsed case.

Ideally, to compare the penetration of a pulsed jet to that of a steady jet, it would be more appropriate to use a pulse-specific VR in the form

$$\mathrm{VR}' = \left(J \Big/ \rho U_\infty^2 A_j\right)^{\frac{1}{2}} \tag{2}$$

where

$$J = \frac{1}{T}\int_0^T \rho u^2(t) A_j \, \mathrm{d}t \tag{3}$$

In this paper, mean or time-averaged VR has been used because instantaneous jet exit velocity has not been measured at the time of this investigation. However, with a constant duty cycle of 50% and with the assumption of perfect square wave form for $u_j(t)$ (without any over- or undershoot), evaluation of VR′ yields VR′ = 1.41VR, independent of pulsing frequency. Inserting this new parameter in the trajectory equation of, for example, Pratte and Baines[11] [Eq. (1)],

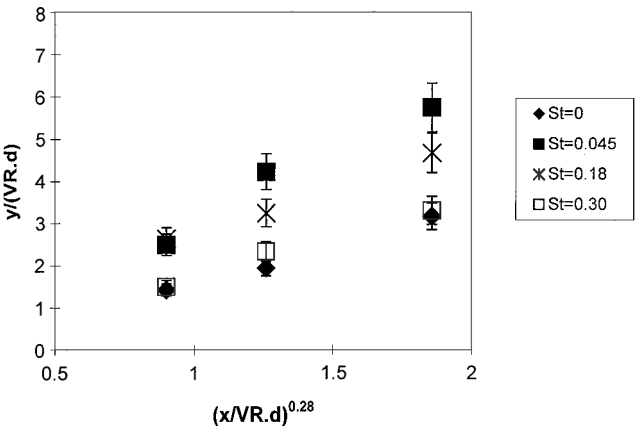

Fig. 9 Normalized penetration depth vs $[x/(\mathrm{VR}d)]^{0.28}$ with Strouhal number as parameter.

yields only a 28% increase in penetration, independent of pulsing frequency, when compared to penetration calculated with time-averaged VR.

The increase in penetration as a result of pulsing, however, is up to 100%, as can be seen in Fig. 7. For this reason, it is reasonable to suggest that an additional mechanism, namely, the spacing of individual vortex rings and the interaction among them, play a decisive role in penetration depth.

C. Entrainment and Mixing

The pulsed jet exhibits two different types of mixing behavior, depending on the flow conditions. During the experiments conducted with a 0.95-cm diameter nozzle, it was observed that, for large values of VR (VR ≥ 5), some portion of the jet fluid is shed into its wake as the rest of it penetrates into the crossflow, for almost the entire range of pulsing frequencies studied. Mixing mechanisms in the wake region and within the jet are different; the wake structure is dominated by vertical columns of vortices, whereas vortex rings created by each pulse are responsible for the entrainment and mixing within the jet. A sample photograph for $Re_j = 3300$, VR = 7.5, and $Sr = 0.4$ is given in Fig 10a, demonstrating this type of behavior by the chemically reacting laser-induced fluorescence technique. The fluid in the wake region does not mix long after the jet itself is completely mixed, as can be seen from this photograph. This is partly due to the vortex structure in the wake and partly because of Reynolds number based on the crossflow speed and jet diameter, that is, wake Reynolds number, is smaller than the Reynolds number of the mixing transition for the flow conditions given earlier. At low values of VR (VR < 5), no jet fluid was observed in the wake as can be seen from Fig. 10b.

Flame length measurements have been conducted by using video recordings of chemically reactive tests. Owing to the passage of large-scale structures, the flame tip position fluctuates periodically. To account for this fluctuaution, at least 10 video frames were used to determine an average flame tip position for each measurement.

Flame length dependency of a pulsed jet of $Re_j = 8{,}000$ on the Strouhal number is given in Fig. 11 for three different VR, including the range of fluctuation. The equivalence ratio ϕ, defined as the volume of crossflow fluid required to completely react with a unit volume of jet fluid, for the pH transition of the indicator was seven during these experiments. When pulsed at low frequencies, a significant reduction in the flame length was observed. That is, at $Sr = 0.1$, the flame length of the pulsed jet was equal to 64, 63, and 51% of its value when the jet was not pulsed for VR = 10, 5, and 3.3, respectively. As the pulsing rate increased beyond $Sr = 0.1$, in all three cases the flame length gradually increased to reach its unforced value.

Ratios of the chord lengths of the flame, defined as $c_f = \sqrt{(x_f^2 + y_f^2)}$, for the pulsed and steady jets are given as a function of the Strouhal number in Fig. 12, for the same flow conditions as in Fig. 11. The greatest effect on mixing due to pulsation was observed for VR = 3.3, about a 40% reduction in the chord length of the flame at $Sr = 0.1$.

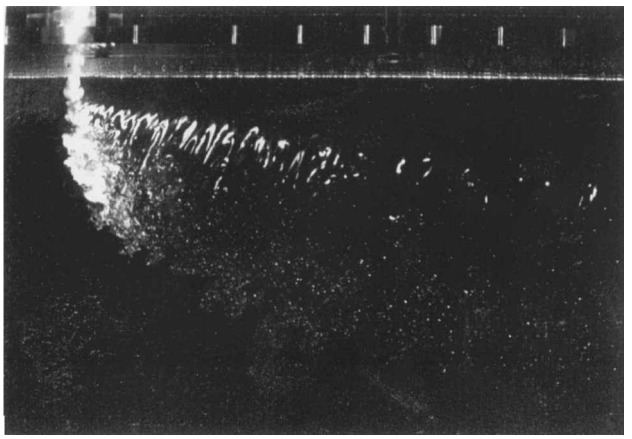

a)

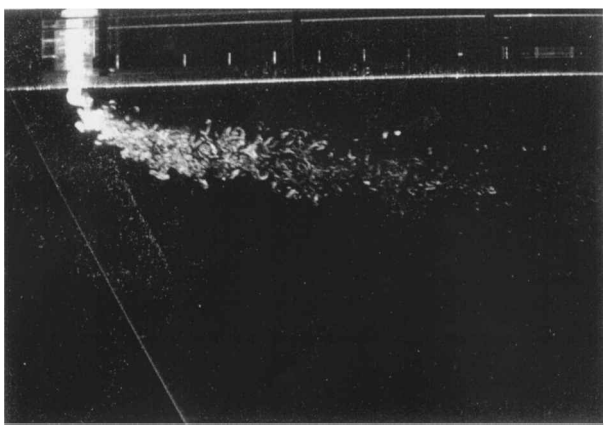

b)

Fig. 10 Flame structure at a) high and b) low VR.

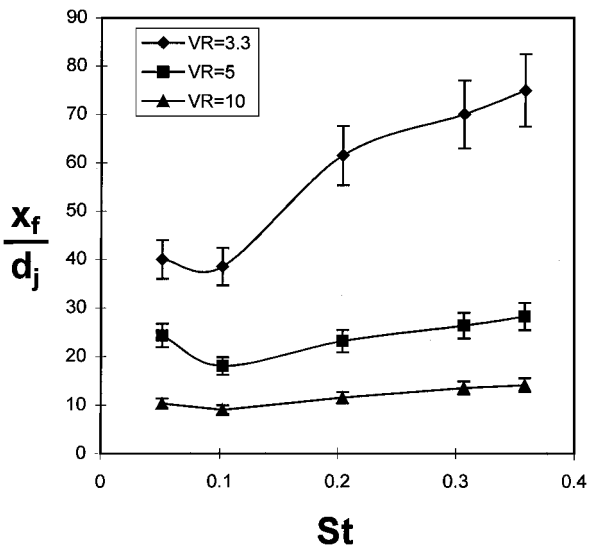

Fig. 11 Flame length vs Strouhal number for $Re_j = 8000$ and $\phi = 7$ (100% modulation).

These measurements may suggest that pulsing has a greater effect on mixing at low VR values. However, it can be also argued that pulsing is more effective on mixing when the steady flame length of the jet is naturally long, due either to low VR or to high equivalence ratio of the chemistry used.

Flow visualization of the jet revealed that pulsation creates distinct vortex rings, which have a lower entrainment rate than a steady jet in crossflow. Only after these discrete rings start interacting can one anticipate a significant improvement in mixing. Thus, it is plausible to expect a greater effect on mixing due to pulsation for flames that extend beyond the jet's near field. In fact, during the preliminary

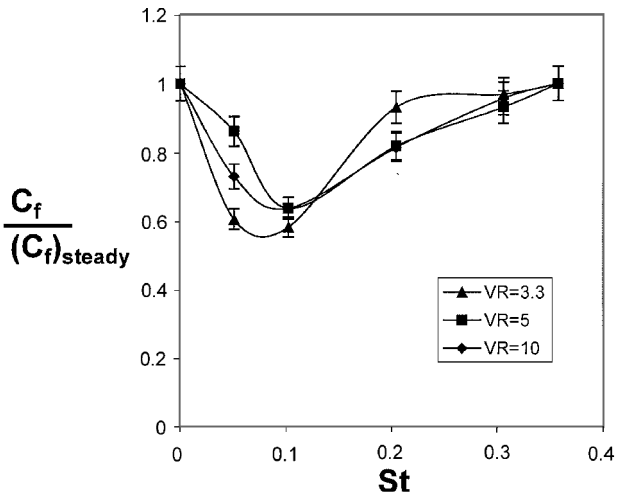

Fig. 12 Flame chord length ratio of pulsed to steady jet vs Strouhal number for $Re_j = 8000$ and $\phi = 7$ (100% modulation).

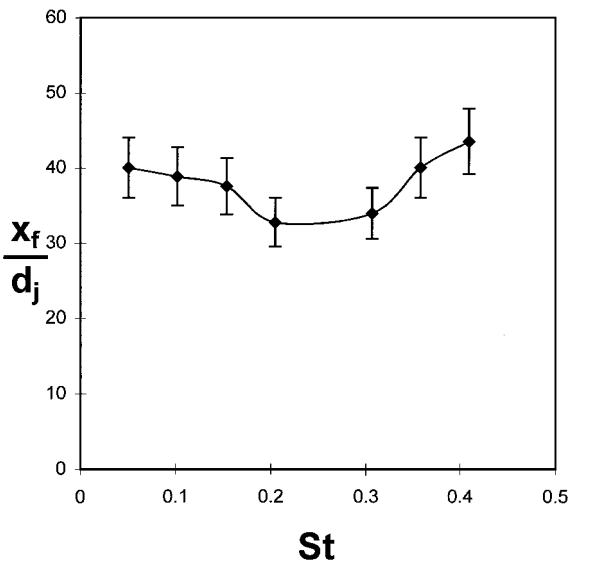

Fig. 13 Flame length vs Strouhal number for $Re_j = 4000$, VR = 2.5, and $\phi = 5.5$ (20% modulation).

experiments conducted with jets of $\phi = 2$, pulsing demonstrated no significant effect on the flame length of the jet.

Also note that the minimum flame length was measured at $Sr = 0.1$ for all three VR values given earlier, indicating that the crossflow velocity does not alter the optimum pulsing frequency for a given jet. Apparently, pulsation creates a near-field vortex rollup that occurs before the crossflow speed U_∞ has an effect.

Then, if the assumption holds that the flame length of the jet is mainly decided by the interactions among neighboring rings, it can also be said that for large values of VR, the optimum pulsing frequency (where the minimum flame length is measured) depends mainly on the jet velocity.

Flame length of a 20% modulated jet as a function of pulsing frequency is given in Fig. 13 for $Re_j = 4000$, VR = 2.5, and $\phi = 5.5$. Experiments suggest a reduced effect on the flame length, compared to fully pulsed jet, when the flow rate of the jet was modulated partially.

IV. Conclusions

Flow visualization experiments with round, turbulent jets in crossflow revealed that structure of a transverse jet is dominated by the formation of a curved shear layer, composed of distinct vortex loops, around the jet in the near-field, as well as the subsequent interactions among neighboring loops as the jet bends over. A unique vortex loop merging pattern was observed that results in cancellation and intensification of the vorticity at different regions of the jet, as certain

parts of the neighboring loops merge with the opposite or the same sign of vorticity, respectively.

Periodic forcing of the jet stream creates vortex loops with their strength and spacing determined by the frequency of the forcing and the jet-to-crossflow VR. By tuning the pulsing frequency for a given jet-to-crossflow VR, it was observed that optimum vortex loop spacing and strength can be achieved that increases the jet's penetration while concurrently enhancing the mixing. Experiments conducted with high-Reynolds-number jets demonstrated up to a 70% increase in penetration depth and a 40% reduction in the chord length or a 50% reduction in the streamwise length of the flame.

It was also observed that, for large values of jet-to-crossflow VR, the optimum pulsing frequency at which penetration and mixing are maximized does not depend on the crossflow velocity.

Chemically reactive experiments also suggest that pulsing has the greatest effect on mixing when the unforced flame extends to the far field. It is suggested that because pulsing creates distinct vortex loops, which have relatively slow entrainment rates until they start pairing, the enhancement associated with pulsing takes place mainly in the far field.

Acknowledgment

This work was supported in part by the Air Force Office of Scientific Research under Grant AFOSR-87-0366.

References

[1]Kamatoni, Y., and Greber, I., "Experiments on a Turbulent Jet in a Cross Flow," *AIAA Journal*, Vol. 10, No. 11, 1972, pp. 1425–1429.

[2]Broadwell, J. E., and Breidenthal, R. E., "Structure and Mixing of a Transverse Jet in Incompressible Flow," *Journal of Fluid Mechanics*, Vol. 148, 1984, pp. 405–412.

[3]Wu, J. M., Vakili, A. D., and Yu, F. M., "Investigation of the Interacting Flow of Nonsymmetric Jets in Crossflow," *AIAA Journal*, Vol. 26, No. 8, 1988, pp. 940–947.

[4]Eroglu, A., and Breidenthal, R. E., "Effects of Periodic Disturbances on Structure and Flame Length of a Jet in Crossflow," AIAA Paper 91-0317, Jan. 1991.

[5]Hermanson, J. C., Wahba, A., and Johari, H., "Duty-Cycle Effects on Penetration of Fully Modulated, Turbulent Jets in Crossflow," *AIAA Journal*, Vol. 36, No. 10, 1998, pp. 1935–1937.

[6]Johari, H., Pacheco-Tougas, M., and Hermanson, J. C., "Penetration and Mixing of Fully Modulated Turbulent Jets in Crossflow," *AIAA Journal*, Vol. 37, No. 7, 1999, pp. 842–850.

[7]Fric, T. F., and Roshko, A., "Vortical Structure in the Wake of a Transverse Jet," *Journal of Fluid Mechanics*, Vol. 279, 1994, pp. 1–47.

[8]Fric, T. F., "Structure in the Near Field of the Transverse Jet," Ph.D. Dissertation, Graduate Aeronautical Labs., California Inst. of Technology, Pasadena, CA, April 1990.

[9]Eroglu, A., "Turbulent Mixing in Accelerating Transverse Jets," AIAA Paper 90-1619, June 1990.

[10]Eroglu, A., and Breidenthal, R. E., "Exponentially Accelerating Jet in Crossflow," *AIAA Journal*, Vol. 36, No. 6, 1998, pp. 1002–1009.

[11]Pratte, B. D., and Baines, W. D., "Profiles of the Round Turbulent Jet in a Cross Flow," *Journal of the Hydronautical Division of the American Society of Civil Engineers*, Vol. 92, Nov. 1967, pp. 53–64.

J. C. Hermanson
Associate Editor